Atmospheric
Chemistry
and Physics
Discussions

# A novel methodology using MODIS and CERES for assessing the daily radiative forcing of smoke aerosols in large scale over the Amazonia

E. T. Sena and P. Artaxo

Institute of Physics, University of São Paulo, São Paulo, Brazil

Correspondence to: E. T. Sena (elisats@if.usp.br)

31515

## Abstract

A new methodology was developed for obtaining daily retrievals of the direct radiative forcing of aerosols (24h-DARF) at the top of the atmosphere (TOA) using satellite remote sensing. For that, simultaneous CERES (Clouds and Earth's Radiant Energy System) shortwave flux at the top of the atmosphere (TOA) and MODIS (Moderate Resolution Spectroradiometer) aerosol optical depth (AOD) retrievals were used. This methodology is applied over a large region of Brazilian Amazonia. We focused our studies on the peak of the biomass burning season (August to September) from 2000 to 2009 to analyse the impact of forest smoke on the radiation balance.

To assess the spatial distribution of the DARF, background scenes without biomass burning impacts, were defined as scenes with MODIS AOD < 0.1. The fluxes at the TOA retrieved by CERES for those clean conditions ($F_{cl}$) were estimated as a function of the illumination geometry ($\theta_0$) for each $0.5° \times 0.5°$ grid cell. The instantaneous DARF was obtained as the difference between clean $F_{cl}$ ($\theta_0$) and the polluted mean flux at the TOA measured by CERES in each cell ($F_{pol}$ ($\theta_0$)). The radiative transfer code SBDART (Santa Barbara DISORT Radiative Transfer model) was used to expand instantaneous DARFs to 24 h averages. With this methodology it is possible to assess the DARF both at large scale and at high temporal resolution. This new methodology also showed to be more robust, because it considerably reduces statistical sources of uncertainties in the estimates of the DARF, when compared to previous assessments of the DARF using satellite remote sensing.

The spatial distribution of the 24h-DARF shows that, for some cases, the mean 24h-DARF presents local values as high as $-30\,\mathrm{W\,m^{-2}}$. The temporal variability of the 24h-DARF along the biomass burning season was also studied and showed large intraseasonal and interannual variability. In an attempt to validate the radiative forcing obtained in this work using CERES and MODIS, those results were compared to coincident AERONET ground based estimates of the DARF. This analysis showed that CERES-MODIS and AERONET 24h-DARF are related as $\mathrm{DARF}_{\mathrm{CERES\text{-}MODIS}}^{24\,\mathrm{h}} =$

31516

$(1.07 \pm 0.04)\text{DARF}_\text{AERONET}^\text{24h} - (0.0 \pm 0.6)$. This is a significant result, considering that the 24h-DARF retrievals were obtained by applying completely different methodologies, and using different instruments. The instantaneous CERES-MODIS DARF was also compared with radiative transfer evaluations of the forcing. To validate the aerosol and surface models used in the simulations, downward shortwave fluxes at the surface evaluated using SBDART and measured by pyranometers were compared. The simulated and measured downward fluxes are related through $F_\text{BOA}^\text{PYRANOMETER} = (1.00 \pm 0.04)F_\text{BOA}^\text{SBDART} - (20 \pm 27)$, indicating that the models and parameters used in the simulations were consistent. The relationship between CERES-MODIS instantaneous DARF and calculated SBDART forcing was satisfactory, with $\text{DARF}_\text{CERES-MODIS} = (0.86 \pm 0.06)\text{DARF}_\text{SBDART} - (6 \pm 2)$. Those analysis showed a good agreement between satellite remote sensing, ground-based and radiative transfer evaluated DARF, demonstrating the robustness of the new proposed methodology for calculated radiative forcing for biomass burning aerosols. To our knowledge, this was the first time satellite remote sensing assessments of the DARF were compared with ground based DARF estimates.

## 1 Introduction

The Amazonia is the largest tropical rainforest of the world, occupying an area of more than 6.6 million km$^2$ in South America. This large ecosystem plays a crucial role in regulating global and regional climate and the hydrological cycle, powering global atmospheric circulation, transporting heat and moisture to continental areas (Artaxo et al., 2013; Davidson and Artaxo, 2004). In the last decades, anthropogenic activities, such as deforestation for agricultural and urban expansion have highly disturbed this important environment (Betts et al., 2008; Bowman et al., 2009; Davidson et al., 2012). During the wet season, the Amazon Basin is one of the few continental places of the world where we can observe pristine conditions (Andreae et al., 2007).

The population of aerosols during the wet season is dominated by primary biogenic coarse mode particles (Martin et al., 2010), and presents typical concentration of about 300 particles cm$^{-3}$ (Artaxo et al., 2002). This scenario changes dramatically during the dry season, with particle concentration reaching around 20 000 particles cm$^{-3}$ due to biomass burning emissions (Andreae et al., 2002; Artaxo et al., 2009; Echalar et al., 1998; Holben et al., 1996). Furthermore, not only does the absolute concentration of particles strongly increases, but there are also tremendous modifications in the size distribution of aerosols, since most of the particles emitted during burning events belong to the fine mode (Dubovik et al., 2002; Eck et al., 2003; Schafer et al., 2008).

Aerosol particles can modify the Earth's radiative balance in two ways: (i) directly, by interacting with solar radiation, through scattering and absorption processes (eg., Charlson et al., 1992; Chylek and Wong, 1995), and (ii) indirectly, by modifying the microphysical structure of clouds, such as droplet size distribution, cloud albedo and other properties (eg., Albrecht et al., 1989; Andreae et al., 2004; Coakley et al., 1987; Koren et al., 2008; Twomey et al., 1977). These effects depend on the concentration and on the horizontal and vertical distributions of particles in the atmosphere, on their optical properties, such as single scattering albedo, size distribution, phase function, hygroscopicity, and on the surface reflectance properties of the underlying region (eg., Haywood and Boucher, 2000; Yu et al., 2006). In particular, biomass burning aerosols play an important role in modifying the radiative energy balance of the affected region because fine mode particles interact efficiently with solar radiation (Liou, 2002).

The direct aerosol radiative forcing (DARF) in Amazonia was previously assessed using radiative transfer models coupled with either ground-based remote sensing (Procopio et al., 2004) or intensive field-campaigns in-situ measurements (Ross et al., 1998). Although these approaches may provide detailed insight about a specific burning event or a bit larger region, they are limited in space (in the case of ground-based studies) or in time (in the case of intensive field campaigns). As satellite remote sensing provides high spatial coverage it has been used to assess the large scale DARF. An interesting technique uses CERES (Clouds and Earth's Radiant Energy System) flux at the

TOA combined with MODIS (Moderate Resolution Spectroradiometer) or MISR (Multi-angle Imaging Spectroradiometer) aerosol optical depth (AOD) to assess the mean DARF over Amazonia during the biomass burning season and analyzes its spatial variability (Patadia et al., 2008; Sena et al., 2013). This technique (CERES+MODIS) has also been widely applied to evaluate the mean DARF over a time period (usually 2–3 months) in several other regions (eg., Christopher, 2011; Zhang et al., 2005; Feng and Christopher, 2014; Sundström et al., 2014). Although these studies focused on averages are useful, they lack the high temporal resolution needed to observe important details on the changes of the radiative balance due to the short residence time of aerosols in the atmosphere. During the dry season, aerosol residence time within the boundary layer is estimated in about 4 to 6 days (Edwards et al., 2006; Freitas et al., 2005). Also, biomass burning aerosols can be transported over great distances away from their sources (Andreae et al., 2001; Longo et al., 2009), depending on the prevalent dynamics in the studied area. Due to their short lifetime and to the dynamics of transport of these particles, aerosols present highly inhomogeneous spatial and temporal distributions. With that in mind, this work has developed a methodology for calculating DARF in Amazonia with higher spatial and temporal resolution than previous assessments ($0.5° \times 0.5°$ and 1 day, respectively) using satellite remote sensing.

The main goals of this work were:

1. to introduce a new methodology to assess the daily direct radiative forcing of biomass burning aerosols in large scale over the Amazonia using satellite remote sensing (Sect. 2);

2. to analyse the intraseasonal and interannual variability of the daily average DARF as well as its mean daily spatial distribution pattern over Amazonia (Sects. 3.1 and 3.2);

3. to validate the calculated DARF obtained by applying this new methodology with ground-based sensors, as well as radiative transfer DARF calculations (Sect. 4).

We also believe that this methodology could be easily applied to study the DARF24h in other regions of the world, impacted by biomass burning or even urban pollution.

## 2   Data and methods

In this work, combined CERES shortwave flux at the top of the atmosphere (TOA) and MODIS aerosol optical depth (AOD) at 550 nm retrievals were used to assess the direct radiative forcing of biomass burning aerosols over the Amazon Basin for cloud-free conditions. Both these instruments are aboard NASA's Terra and Aqua satellites.

CERES sensors are passive scanning radiometers that measure the upward radiance in three broadband channels: (i) between 0.3 to 5.0 µm, to measure the shortwave radiation reflected in the solar spectrum, (ii) between 8 and 12 µm, to measure the thermal radiation emitted by the Earth in the atmospheric window spectral region, and (iii) between 0.3 and 200 µm to measure the total radiation spectrum emerging at the TOA (Wielicki et al., 1996). Radiance measurements are converted into broadband radiative fluxes through the use of angular distribution models (ADMs) (Loeb et al., 2005).

MODIS sensor measure the radiance at the TOA in 36 narrow spectral bands between 0.4 and 14.4 µm (Salomonson et al., 1989). Among its various applications, MODIS observations have been widely used to monitor land surface, oceans and atmosphere properties and to provide information about clouds and aerosols optical properties, their spatial and temporal variations, and the interaction between aerosols and clouds (King et al., 1992).

CERES Single Scanner Footprint (CERES-SSF) product provides simultaneous retrievals of the upward flux at the TOA derived by CERES on three broadband channels, and properties of aerosols and clouds reported by MODIS. In this product, MOD04 aerosol and clouds properties, that are originally reported with a 10 km spatial resolution, are reprojected to CERES 20 km resolution (Smith, 1994). Over land, MODIS's AOD uncertainty is estimated as: $\sigma_{land} = \pm 0.05 \pm 0.15 \, AOD_{550\,nm}$ (Remer et al., 2005).

For the development of the new methodology presented here, we used CERES-SSF Edition 3A shortwave flux at the TOA retrievals from Terra satellite over the Amazon Basin from 1 July to 31 October from 2000 to 2009. The studied area was limited between the coordinates 3° N–20° S, 45–65° W and 3° N–11° S, 65–74° W. Pixels with 1 km resolution MODIS cloud fraction above 0.5 % and with a clear area in the MODIS 250 m resolution lower than 99.9 % were removed. To limit distortions we removed from our analysis pixels that presented view and solar zenith angles greater than 60°. The DARF was calculated with a 0.5° × 0.5° latitude/longitude spatial resolution, according to the methodology described in the next section.

## 2.1 Evaluation of the daily direct RF of biomass burning aerosols

The direct radiative forcing of aerosols (DARF) can be defined as the difference between the upward radiation flux at the TOA measured in background conditions ($F_{cl}$) and in polluted conditions ($F_{pol}$).

$$DARF = F_{cl} - F_{pol}. \tag{1}$$

For each scene observed by CERES, $F_{pol}$ can be obtained directly from the mean flux at the TOA for each 0.5° × 0.5° grid cell. To calculate the instantaneous DARF, we need to estimate what would be the flux at the TOA for background conditions ($F_{cl}$) for the same illumination geometry of the polluted scene. To perform this estimate, scenes that presented aerosol optical depth (AOD) smaller than 0.1 were selected, and considered as background scenes. For each cell, the flux at the TOA observed for background scenes ($F_{cl}$) during the 40 months studied period was plotted against the cosine of the solar zenith angle ($\cos(\theta_0)$). An example of this plot, for the grid cell centred at latitude 8.75° S and longitude 53.75° W, is shown in Fig. 1. A correlation coefficient of 0.94 between $F_{cl}$ and $\cos(\theta_0)$ was observed for the data points within this cell indicating the adequacy of the linear aproximation.

The solar zenith angle varied from about 10 to 52° at Terra satellite passage time over the Amazonia during the studied period. For this solar zenith angle range, $F_{cl}$ varies

linearly with $\cos(\theta_0)$. By adjusting a linear fit to the data points within each cell we can calculate $F_{cl}(\theta_0)$ for any illumination geometry, according to Eq. (2),

$$F_{cl}(\theta_0) = A\cos(\theta_0) + B, \tag{2}$$

where $A$ and $B$ correspond to the slope and the intercept of the linear fit, respectively.

To assess the instantaneous DARF, the mean solar zenith angle within each cell during the satellite passage time was identified for every polluted scene. For each cell, the instantaneous DARF was evaluated as the difference between $F_{cl}(\theta_0)$ and the mean flux at the TOA retrieved by CERES in polluted conditions ($F_{pol}(\theta_0)$), as previously stated in Eq. (1). The uncertainty of the DARF in each cell ($\sigma_{DARF}$), was computed using error propagation, according to the following equation:

$$\sigma_{DARF}^2 = \sigma_A^2 \cos^2(\theta_0) + \sigma_B^2 + 2\text{cov}(A,B)\cos(\theta_0) + \sigma_{Fpol}^2, \tag{3}$$

where $\sigma_A$, $\sigma_B$ and $\text{cov}(A,B)$ are the uncertainty of the slope, intercept and the covariance between the slope and the intercept, respectively; $\sigma_{Fpol}$ is the uncertainty of the of the flux in each cell for the polluted condition.

## 2.2 Correction of the DARF according to empirical ADMs

As already discussed, to convert CERES radiances measurements to radiative flux at the TOA it is necessary to define the angular distribution models (ADMs) for different scenes (Loeb et al., 2005). In a recent work, Patadia et al. (2011) pointed out that the angular distribution models currently used by CERES team to derive shortwave fluxes at the TOA over land in cloud-free conditions do not take into account aerosol properties in the observed scene. This can result in large errors in the shortwave fluxes derived by this sensor for areas with high concentrations of aerosols, such as the Amazonia during the biomass burning season. To estimate the impact of the anisotropy caused by high aerosol loading on the flux at the TOA, Patadia et al. (2011) developed a methodology to obtain new empirical angular distribution models for the

Amazon Basin region during the dry season. For this, the authors used radiance measurements obtained by CERES shortwave channel over the Amazonia for different view and solar illumination geometries between 2000 and 2008. In a later work they have assessed the difference between the DARF evaluated using both, CERES ADMs and their new empirical ADMs (Patadia and Christopher, 2014). They have found that, on average, CERES DARF relates to the corrected DARF calculated with their empirical ADMs, according to the following equation:

$$DARF_{corrected} = DARF - 52.27AOD - 2.71 + 35.15AOD + 1.78. \qquad (4)$$

The correction proposed by Patadia and Christopher (2014) was applied to the CERES-MODIS DARF estimates introduced in the previous section.

A discrete-ordinate radiative transfer (DISORT) code (Stamnes et al., 1988) was used to expand the instantaneous radiative forcing, calculated for the satellite passage time, to 24 h averages. MODIS BRDF/Albedo Model (MCD43B1) retrievals (Schaaf et al., 2002) over the studied area were used to develop the surface albedo models used in the radiative transfer calculations. Aerosol optical properties retrieved by the AERONET (Aerosol Robotic Network) ground-based sun-photometers (Dubovik and King, 2000) located in the Amazonia during the dry season were also used in this computation. For a detailed description of the methodology used to perform this expansion please refer to Sena et al. (2013).

## 3 Results and discussions

In this section we will present and explore the main results obtained by applying the methodology introduced in Sect. 2.1 to assess the DARF. Some examples of the spatial distribution and the temporal variability of the 24h-DARF along the biomass burning season are shown and discussed in the next subsections. In Sect. 3.3, the average of the DARF during the biomass burning season of each year is computed and compared with previous DARF results.

### 3.1 Examples of the spatial distribution of the 24h-DARF

Aerosols can be transported over long distances away from their sources and, therefore, can cover large areas (Prins et al., 1998). Two examples of the spatial distribution of the 24h-DARF, for 13 and 15 August 2005, are shown in Fig. 2, with their respective uncertainties. Composite images from MODIS's red, blue and green spectral channels, are also shown in this figure.

Figure 2 shows that, on 13 August 2005, the smoke plume covers a large area of the Brazilian Amazonia, between 4 and 12° S and 55 and 70° W. The 24h-DARF over the area was particularly high for that day, varying from about $-15$ to $-30\,W\,m^{-2}$. On 15 August 2005, we note that the smoke plume has moved Southeast, following the Andes mountain range line, strongly impacting the Southern Amazonia, Western Bolivia and Northern Paraguay. The area located between 8 and 20° S and 57 and 65° W showed the highest 24h-DARF values for that day, also ranging from $-15$ to $-30\,W\,m^{-2}$. The 24h-DARF showed in Fig. 2b was, on average, $-14.3 \pm 0.3\,W\,m^{-2}$ on 13 August and $-15.6 \pm 0.3\,W\,m^{-2}$ on 15 August. These results clearly show the importance of wind circulation in the transport of aerosol plumes and how atmospheric dynamics may influence the shortwave radiative balance of the region.

### 3.2 Temporal variability of the DARF along the biomass burning season

Due to the short lifetime of aerosols in the atmosphere, the DARF may vary largely along the 2 months of the biomass burning season. To analyze this temporal variability, the average of the 24h-DARF over the studied area was calculated for each day of the year. Examples of the time series of the mean daily DARF during the biomass burning season of 2005, 2006 and 2007 are illustrated in Fig. 3.

Figure 3 shows that, besides its large interannual variability, the DARF also varies widely along the biomass burning season. Different temporal patterns along the biomass burning season are observed depending on the year. For example, for most of 2005's dry season, the DARF showed little variation, averaging around $-9 \pm 2\,W\,m^{-2}$.

On the other hand, in 2007, the DARF became gradually more negative, starting around $0\,W\,m^{-2}$ in the beginning of August and reaching values of the order of $-25\,W\,m^{-2}$ at the end of September. However, 2005 and 2007, both, present similar mean 24h-DARF during the burning season, as will be shown in the next section (Fig. 5). The temporal variation pattern during the biomass burning season of 2006 presents an intermediate trend to those observed in 2005 and 2007. That is, the DARF becomes more negative until the beginning of September, when it saturates and finally turns less negative. The DARF variations from one day to the other, shown in these figures, are due to changes in cloudiness and at the area scanned by MODIS, that varies according to the satellite track.

### 3.3 Average of the DARF during the biomass burning season

In previous studies (Patadia et al., 2008; Sena et al., 2013), the average of the direct radiative forcing of aerosols during the biomass burning season over the Amazonia was also calculated using CERES and MODIS sensors. In those approaches, the average flux for clean conditions during the biomass burning season (BBSF$_{cl}$) for each cell grid was estimated from the intercept of the regression between TOA fluxes and AOD retrievals from August to September (Fig. 4). The mean DARF during the biomass burning season (BBSDARF) was then calculated by subtracting the mean flux at the TOA (BBSF$_{pol}$) from the mean flux for clean conditions (BBSF$_{cl}$) observed as averages during the two-months studied period.

The new methodology introduced here (Sect. 2.1), provides the 24h-DARF for each individual day of the year, that is, in a much higher temporal resolution than the one used in previous studies. In this section we aim to compare the DARF obtained using the new methodology introduced in Sect. 2.2 with the seasonal DARF values calculated previously by Sena et al., 2013. For this comparison, the daily DARF, obtained in this work, was averaged between the months of August and September of each year ($\langle24hDARF\rangle_{BBS}$). To ensure that we make a fair comparison, the corrections proposed by Patadia and Christopher (2014), and used for the evaluation of the 24h-DARF in

this paper (Sect. 2.2), were also applied a posteriori to the Sena et al., 2013 seasonal forcing (BBSDARF). Figure 5 shows the mean AOD at 550 nm during the biomass burning, and the comparison between $\langle24hDARF\rangle_{BBS}$ and BBSDARF, calculated over the studied area, from 2000 to 2009.

Figure 5 shows that the $\langle24hDARF\rangle_{BBS}$ is consistently lower than the BBSDARF. The average of the BBSDARF for this 10 year period (2000 to 2009) was $-8.2 \pm 2.1\,W\,m^{-2}$, while the 10 year average of the $\langle24hDARF\rangle_{BBS}$ was smaller at $-5.2 \pm 2.6\,W\,m^{-2}$. Part of this difference may be explained by the different references used for the evaluation of the flux for clean conditions. In the old methodology used by Sena et al., 2013, BBSF$_{cl}$ was defined considering AOD = 0, since the clean condition was chosen as the intercept between fluxes and AOD = 0. This methodology leads to the effect that the contribution of background aerosols (AOD approximately 0.1) was not accounted for in the final evaluation of BBSDARF. On the other hand, in the new methodology introduced here, $F_{cl}$ was defined specifically for more realistic background conditions, according to Sect. 2.1. Therefore, it was expected that the $\langle24hDARF\rangle_{BBS}$ would be less negative than the BBSDARF. Radiative transfer calculations done with SBDART (Santa Barbara DISORT Radiative Transfer model) (Richiazzi et al., 1998) suggest that the contribution of background aerosols at AOD = 0.1 to the 24h-DARF over the Amazonia is about $-2\,W\,m^{-2}$. Therefore, the contribution of background aerosols may explain the magnitude of the differences in the radiative forcings obtained from 2005 on, but not before that year. Part of the DARF differences observed from 2000 to 2003, are most certainly associated with the aerosol optical properties contained in CERES-SSF product, Edition 3A, that was used both in this work and by Sena et al. (2013). This product provides aerosol optical properties calculated using MODIS aerosol algorithm MOD04 – collection 4 until mid-2005, and MOD04 – collection 5 after that date. A major difference between the optical depths obtained by these two collections, is the fact that collection 4 does not allow negative values of AOD, while for collection 5, the lowest limit for the AOD is $-0.05$, to account for the uncertainty of the retrieved AOD. Therefore, for low aerosol loading, when AOD from MOD04 – collection 4 is projected to CERES

lower resolution, it may be overestimated, since negative AOD values were removed from the average. Thus, when applying the methodology used by Patadia et al. (2008) and Sena et al. (2013), to CERES-SSF data that contained MOD04 – collection 4 AOD, the $BBSF_{cl}$ is underestimated and, therefore, the BBSDARF is overestimated (Fig. 6). This explains the differences between both DARF evaluations observed in Fig. 5.

The solar zenith angle strongly influences the upward flux at the TOA ($F_{TOA}$). CERES fluxes retrievals obtained over the same surface, for the same aerosol loading and same atmospheric conditions, and at different illumination geometry will present different $F_{TOA}$. In the previous methodology used in Sena et al., 2013, two months of data were used to estimate the BBSDARF through the linear fit of $F_{TOA}$ by AOD. Thus, flux measurements performed on different days and at different times (and therefore different solar zenith angles) contributed to increase the dispersion of the points on the $y$ axis, increasing the uncertainty of BBSDARF (Fig. 4). In the new methodology, the DARF is obtained as a function of the solar zenith angle, which eliminates the noise caused by solar zenith angle variations, observed in previous studies. This was another important improvement of the methodology proposed in this work over the previously used methodology.

The mean correlations between the AOD 550 nm and the $\langle 24hDARF \rangle_{BBS}$ from 2000 to 2009 was $-0.86 \pm 0.03$, higher than the mean correlations between the AOD and BBSDARF previously obtained, of $-0.75 \pm 0.05$. This is another indication that the new daily methodology proposed here is more robust to evaluate the DARF than the seasonal averaged methodology used in previous studies.

## 4 Validation of aerosol radiative forcing

The methodology proposed in this work uses upward TOA fluxes estimates from CERES-MODIS sensors aboard Terra for evaluating the DARF over the Amazonia and cerrado regions. As CERES rely on angular distribution models (ADM) for estimating the upward flux at the TOA, it is very hard to really validate those flux retrieval. Up to

date, the validation of these TOA fluxes has only been made indirectly, by comparing TOA fluxes retrieved by broadband radiometers aboard different satellites (Loeb et al., 2007). As previously discussed, the use of different ADMs to convert broadband radiance measurements into flux may introduce large differences in the DARF calculated using satellite remote sensors (Patadia and Christopher, 2014). We have applied a correction to the DARF based on Patadia et al. (2011) empirical ADMs that account for the influence of aerosols in the anisotropy of scattered radiation. Nevertheless, those new angular distribution functions are also not validated and, since there are no instruments that directly measure the upward flux at the TOA, it is not possible to truly validate neither CERES ADMs nor Patadia's empirical ADMs.

As an attempt to indirectly validate the DARF results obtained here, we compared the DARF, calculated in this work, with both ground-based measurements and radiative transfer models forcing estimates. In Sect. 4.1 we analyzed the intercomparison between CERES-MODIS forcings, with those reported by AERONET's (AErosol RObotic NETwork) radiative forcing product. In Sect. 4.2, CERES-MODIS forcings are also compared with radiative forcing evaluations computed using SBDART (Santa Barbara DISORT Atmospheric Radiative Transfer model) radiative transfer code (Richiazzi et al., 1998).

### 4.1 Intercomparison between CERES-MODIS and AERONET 24h-DARF

AERONET is one of the most successful ground-based global networks of sun/sky radiometers for studying and monitoring aerosol physical properties around the world (Holben et al., 1998). Direct and almulcantar measurements from AERONET radiometers are used to retrieve the AOD and several column averaged aerosol optical and physical properties in different spectral bands. Extinction measurements on the spectral channel centered at 940 nm are used to assess column water vapour (Halthore et al., 1997). In its inversion product version 2.0, AERONET provides cloud-free sky DARF estimates. These DARF estimates are evaluated using the radiative transfer code GAME (Global Atmospheric Model) (Dubuisson et al., 1996). The aerosol and

surface models used in GAME are based on mean column averaged aerosol optical properties retrieved by AERONET's inversion algorithm (Dubovik and King, 2000) and surface properties retrieved by MODIS bidirectional reflectance product (Lucht et al., 2000; Schaaf et al., 2002), respectively.

The CERES-MODIS DARF, calculated according to the methodology described in Sect. 2.1, was compared with the DARF reported by AERONET's inversion product. For this, we selected forcing results, located within ±25 km of the AERONET sites that were operating in the Amazonia during the studied period (Abracos Hill, Alta Floresta, Balbina, Belterra, Cuiabá, Ji-Paraná and Rio Branco). AERONET sunphotometers, only perform the almulcantar measurements, needed to calculate the radiative forcing when the solar zenith angle is larger than 50°. However, during the dry season, at the time Terra overpasses the studied region (around 10:30 LT), the solar zenith angle is on average around 33°. For this reason, there were no coincident instantaneous DARF retrievals from CERES-MODIS radiometers and AERONET sunphotometers. To compare the results, the instantaneous DARF, obtained by both CERES-MODIS and AERONET, were expanded to 24 h average DARF using the methodology described in Sena et al., 2013. A comparison between the 24h-DARF at the TOA obtained using AERONET and CERES-MODIS is shown in Fig. 7.

By applying a linear fit to the data points of Fig. 7, we see that the 24h-DARF derived from CERES-MODIS relates with the 24h-DARF reported by AERONET through the following equation:

$$\text{DARF}^{24\,h}_{\text{CERES-MODIS}} = (1.07 \pm 0.04)\text{DARF}^{24\,h}_{\text{AERONET}} - (0.0 \pm 0.6). \tag{5}$$

According to this equation, the slope of the regression is compatible with 1 within 2 uncertainties and the intercept is zero. This is a remarkable result, since the 24h-DARF retrievals, showed in Fig. 7, were obtained by applying completely different methodologies, and using different instruments. AERONET sunphotometers were at ground level, and CERES-MODIS were at 705 km, aboard Terra satellite both looking at the atmospheric column. Besides that, as explained above, the instantaneous observations

31529

that were used to calculate the 24h-DARF, compared in our analysis, were performed at different hours of the day. All those differences contribute to the dispersion of about $5\,\text{W}\,\text{m}^{-2}$ around the adjusted line. The uncertainties involved in the surface and aerosol optical models used in GAME's radiative transfer code to calculate the DARF reported by AERONET can also contribute somewhat to this dispersion. These results indicate a high agreement between the 24h-DARF obtained by these two independent procedures.

## 4.2 Intercomparison between CERES-MODIS and SBDART instantaneous DARF

It is important to intercompare satellite remote sensing retrievals with ground based measurements. In order to properly do that it was compared CERES-MODIS determinations at the TOA with SolRad-NET (Solar Radiation Network) pyranometers at the bottom of the atmosphere (BOA), using SBDART calculations to link BOA to TOA. To formulate the surface models used in SBDART, we selected 50 km × 50 km areas centred at the AERONET stations, listed in Sect. 4.1. For each selected area, the spectral surface albedo was obtained from the linear interpolation of MODIS MCD43B1 surface albedo retrievals in 7 wavelengths (Lucht et al., 2000; Schaaf et al., 2002). Daily averages of aerosol optical properties retrieved by AERONET inversion product were used to define the aerosol models used in these simulations. The aerosol optical depth and column water vapour measured by AERONET sunphotometers within ±1/2 h of Terra's timepass over each site were also used as inputs in the radiative transfer code. The shortwave downward flux at the surface and the DARF at the TOA were computed with SBDART and compared with ground-based sensors solar flux measurements and with CERES-MODIS DARF, respectively.

Figure 8 shows the comparison between the downward flux at the surface ($F_{\downarrow\text{BOA}}$) calculated by SBDART between 0.3 and 2.8 μm and coincident solar flux measurements at the surface in the same spectral range from SolRad-NET pyranometers, that are collocated with AERONET sunphotometers. A linear fit of the downward flux measured by the pyranometer at the surface ($F^{\text{PYRANOMETER}}_{\text{BOA}}$) and calculated by SBDART

31530

$(F_{\text{BOA}}^{\text{SBDART}})$ indicate that these variables are related through the following equation:

$$F_{\text{BOA}}^{\text{PYRANOMETER}} = (1.00 \pm 0.04)F_{\text{BOA}}^{\text{SBDART}} - (20 \pm 27). \qquad (6)$$

According to the adjusted parameters of this fit and their uncertainties, the slope and intercept of the linear fit (Eq. 6) are compatible with 1 and 0, respectively, within one uncertainty. The apparent mismatch of about $20\,\text{W\,m}^{-2}$ between the calculated and measured values represents approximately 2.2 % of the downward flux at the surface, and this is close to the instrumental uncertainty of the pyranometer, reported as 2 %. These results show a good agreement between the downward irradiance at the surface, calculated using SBDART and SolRad-NET pyranometers measurements.

The intercomparison between the instantaneous TOA DARF obtained using CERES-MODIS and calculated using SBDART is shown in Fig. 9. The data points in this graph have a dispersion of about $10\,\text{W\,m}^{-2}$ around the 1 : 1 line. A linear fit of the data plotted in Fig. 9 shows that the instantaneous TOA DARF obtained from CERES-MODIS and from SBDART relate through the following equation:

$$\text{DARF}_{\text{CERES-MODIS}} = (0.86 \pm 0.06)\text{DARF}_{\text{SBDART}} - (6 \pm 2), \qquad (7)$$

indicating that the curve obtained by linear regression of the points is close to $y = x$ line for the range of values analysed.

Several issues in this comparison must be taken into account. First the upward flux is strongly influenced by the surface reflection. MODIS sensor presents low spectral resolution in the shortwave spectrum and this limits the surface albedo model used as input in SBDART. Secondly, the atmosphere has to be taken into account twice: on the downward and upward path. This amplifies any inaccuracy in the optical properties assumed in the SBDART calculations.

Small deviations in the estimates of aerosol single scattering albedo can generate large differences in the forcing calculated by radiative transfer codes (Loeb and Su, 2010; Boucher et al., 2013). To assess the impact of the uncertainties associated with

different single scattering albedo values, the 24h-DARF was computed in SBDART as a function of AOD at 550 nm for different values of single scattering albedo at 440 nm ($\omega_0 = 0.89$, 0.92 and 0.95) (Fig. 10). The differences of $\pm0.03$ for $\omega_0$, used in these simulations, correspond to the uncertainty of the single scattering albedo inverted by the AERONET algorithms. According to Fig. 10, a variability of 0.03 in the estimate of the single scattering albedo can generate a difference in the computed 24h-DARF of about 5 to $6\,\text{W\,m}^{-2}$ when AOD = 1 and 12 to $14\,\text{W\,m}^{-2}$ when AOD = 5. These values are very significant, and shows that the critical parameter in assessing the correct DARF is actually the aerosol single scattering albedo.

Considering all potential sources of uncertainties on the aerosol and surface albedo models used in SBDART simulations on computing DARF, it is possible to consider the validation showed on Fig. 9 as satisfactory. It is important to note that this validation consist of an indirect comparison, since, as previously discussed, it is not possible to obtain the flux at the TOA by direct methods.

## 5 Summary and conclusions

This work proposed a new methodology for assessing the direct radiative forcing of biomass burning aerosols in large scale over the Amazonia using satellite remote sensing. Ten years of simultaneous CERES and MODIS retrievals, from 2000 to 2009, were used in this evaluation. An important correction (Patadia and Christopher, 2014) was applied to the DARF, to account for the anisotropic scattering of smoke aerosols.

The spatial and temporal distributions of the mean daily DARF were analysed. Those analysis showed that due to the wind dynamics and fast transport of particles along the Amazon Basin, the spatial distribution of the DARF may considerably change even during short periods of time. The DARF varies strongly along the biomass burning season, showing up to $20\,\text{W\,m}^{-2}$ daily variation. The intraseasonal behaviour of the DARF also varied significantly from year to year due to different burning intensity associated

with different climatic conditions and other socioeconomical changes (Davidson et al., 2012).

The average of DARF during the biomass burning season were computed and compared with DARF results obtained in a previous study (Sena et al., 2013). This comparison showed a mean difference of about $3\,\mathrm{W\,m^{-2}}$ on the DARF, depending on the methodology applied. This difference was mainly caused by two factors: (i) the difference in the reference used to represent the clean scene in these two methodologies, and (ii) the fact that, before 2005, CERES-SSF product contains properties of aerosols from an older MODIS collection (collection 4), which overestimates the forcing computed for those years when the previous methodology in applied.

An important part of our efforts focused on linking satellite remote sensing with ground based aerosol and radiation flux measurements. The intercomparison between DARF results assessed using the new methodology proposed in this work, AERONET and SBDART were very satisfactory. This validation also indicates the importance of taking into account the angular distribution model corrections proposed by Patadia and Christopher, 2014, and used in the present study. To our knowledge, this was the first time satellite remote sensing assessments of the DARF were compared with ground based DARF estimates.

The new methodology introduced in this work assesses the radiative forcing of biomass burning aerosols over the Amazonia in large scale and at higher temporal resolution than previous studies. It also shows an advantage over previous approaches for evaluating the DARF using satellite remote sensing, because it considerably decreases the statistical noise in the estimates of the DARF, resulting in higher correlation between DARF and AOD, compared to previous assessments. This new methodology could also be applied to assess the DARF in other places of the world under urban or biomass burning aerosol influences, if suitable and robust aerosol optical parameters are available.

31533

## References

Albrecht, B. A.: Aerosols, cloud microphysics, and fractional cloudiness, Science, 245, 1227–1230, 1989.

Andreae, M. O.: Aerosols before pollution, Science, 315, 50–51, 2007.

Andreae, M. O., Artaxo, P., Fischer, H., Freitas, S. R., Grégoire, J. M., Hansel, A., Hoor, P., Kormann, R., Krejci, R., Lange, L., Lelieveld, J., Lindinger, W., Longo, K., Peters, W., de Reus, M., Scheeren, B., Dias, M., Strom, J., van Velthoven, P. F. J., and Williams, J.: Transport of biomass burning smoke to the upper troposphere by deep convection in the equatorial region, Geophys. Res. Lett., 28, 951–954, doi:10.1029/2000GL012391, 2001.

Andreae, M. O., Artaxo, P., Brandao, C., Carswell, F. E., Ciccioli, P., da Costa, A. L., Culf, A. D., Esteves, J. L., Gash, J. H. C., Grace, J., Kabat, P., Lelieveld, J., Malhi, Y., Manzi, A. O., Meixner, F. X., Nobre, A. D., Nobre, C., Ruivo, M., Silva-Dias, M. A., Stefani, P., Valentini, R., von Jouanne, J., and Waterloo, M. J.: Biogeochemical cycling of carbon, water, energy, trace gases, and aerosols in Amazonia: the LBA-EUSTACH experiments, J. Geophys. Res.-Atmos., 107, 8066, doi:10.1029/2001JD000524, 2002.

Andreae, M. O., Rosenfeld, D., Artaxo, P., Costa, A. A., Frank, G. P., Longo, K. M., and Silva-Dias, M. A. F.: Smoking rain clouds over the Amazon, Science, 303, 1337–1342, 2004.

Artaxo, P., Martins, J. V., Yamasoe, M. A., Procopio, A. S., Pauliquevis, T. M., Andreae, M. O., Guyon, P., Gatti, L. V., and Leal, A. M. C.: Physical and chemical properties of aerosols in the wet and dry seasons in Rondonia, Amazonia, J. Geophys. Res.-Atmos., 107, LBA 49-1–LBA 49-14, doi:10.1029/2001JD000666, 2002.

Artaxo, P., Rizzo, L. V., Paixao, M., de Lucca, S., Oliveira, P. H., Lara, L. L., Wiedemann, K. T., Andreae, M. O., Holben, B., Schafer, J., Correia, A. L., and Pauliquevis, T. M.: Aerosol par-

31534

ticles in Amazonia: their composition, role in the radiation balance, cloud formation, and nutrient cycles, Geoph. Monog. Series, 186, 233–250, doi:10.1029/2008GM000778, 2009.

Artaxo, P., Rizzo, L. V., Brito, J. F., Barbosa, H. M. J., Arana, A., Sena, E. T., Cirino, G. G., Bastos, W., Martin, S. T., and Andreae, M. O.: Atmospheric aerosols in Amazonia and land use change: from natural biogenic to biomass burning conditions, Faraday Discuss., 165, 203–235, doi:10.1039/C3FD00052D, 2013.

Betts, R. A., Malhi, Y., and Roberts, J. T.: The future of the Amazon: new perspectives from climate, ecosystem and social sciences, Philos. T. R. Soc. B, 363, 1729–1735, 2008.

Boucher, O., Randall, D., Artaxo, P., Bretherton, C., Feingold, G., Forster, P., Kerminen, V.-M., Kondo, Y., Liao, H., Lohmann, U., Rasch, P., Satheesh, S. K., Sherwood, S., Stevens, B., and Zhang, X. Y.: Clouds and aerosols, in: Climate Change 2013: The Physical Science Basis. Contribution of Working Group I to the Fifth Assessment Report of the Intergovernmental Panel on Climate Change, edited by: Stocker, T. F., Qin, D., Plattner, G.-K., Tignor, M., Allen, S. K., Boschung, J., Nauels, A., Xia, Y., Bex, V., and Midgley, P. M., Cambridge University Press, Cambridge, UK, New York, NY, USA, 571–657, 2013.

Bowman, D. M. J. S., Balch, J. K., Artaxo, P., Bond, W. J., Carlson, J. M., Cochrane, M. A, D'Antonio, C. M., Defries, R. S., Doyle, J. C., Harrison, S. P., Johnston, F. H., Keeley, J. E., Krawchuk, M. A., Kull, C. A., Marston, J. B., Moritz, M. A., Prentice, I. C., Roos, C. I., Scott, A. C., Swetnam, T. W., van der Werf, G. R., and Pyne, S. J.: Fire in the Earth system, Science, 324, 481–484, doi:10.1126/science.1163886, 2009.

Charlson, R. J., Schwartz, S. E., Hales, J. M., Cess, R. D., Coakley, J. J., Hansen, J. E., and Hofmann, D. J.: Climate forcing by anthropogenic aerosols, Science, 255, 423–430, 1992.

Christopher, S. A.: Satellite remote sensing methods for estimating clear sky shortwave top of atmosphere fluxes used for aerosol studies over the global oceans, Remote Sens. Environ., 115, 3002–3006, 2011.

Chylek, P. and Wong, J.: Effect of absorbing aerosols on global radiation budget, Geophys. Res. Lett., 22, 929–931, 1995.

Coakley, J. A., Bernstein, R. L., and Durkee, P. A.: Effect of ship-stack effluents on cloud reflectivity, Science, 237, 1020–1022, 1987.

Davidson, E. A. and Artaxo, P.: Globally significant changes in biological processes of the Amazon Basin: results of the Large-scale Biosphere–Atmosphere Experiment, Glob. Change Biol., 10, 1–11, doi:10.1111/j.1529-8817.2003.00779.x, 2004.

Davidson, E. A., Araújo A. C., Artaxo, P., Balch, J. K., Brown, I. F., Bustamante, M. M. C., Coe, M. T., DeFries R. S., Keller M., Longo M., Munger J. W., Schroeder W., Soarez-Filho B. S., Souza C. M., and Wofsy S. C.: The Amazon Basin in transition, Nature, 481, 321–328, doi:10.1038/nature10717, 2012.

Dubovik, O. and King, M. D.: A flexible inversion algorithm for retrieval of aerosol optical properties from Sun and sky radiance measurements, J. Geophys. Res., 105, 20673–20696, doi:10.1029/2000JD900282, 2000.

Dubovik, O., Holben, B., Eck, T., Smirnov, A., Kaufman, Y., King, M., Tanré D., and Slutsker, I.: Variability of absorption and optical properties of key aerosol types observed in worldwide locations, J. Atmos. Sci., 59, 590–608, 2002.

Dubuisson, P., Buriez. J. C., and Fouquart, Y.: High spectral resolution solar radiative transfer in absorbing and scattering media: application to the satellite simulation, J. Quant. Spectrosc. Ra., 55, 103–126, 1996.

Echalar, F., Artaxo, P., Martins, J. V., Yamasoe, M., Gerab, F., Maenhaut, W., and Holben, B.: Long-term monitoring of atmospheric aerosols in the amazon basin: source identification and apportionment, J. Geophys. Res., 103, 31849–31864, 1998.

Eck, T. F., Holben, B. N., Reid, J. S., O'Neill, N. T., Schafer, J. S., Dubovik, O., Smirnov, A., Yamasoe, M. A., and Artaxo, P.: High aerosol optical depth biomass burning events: a comparison of optical properties for different source regions, Geophys. Res. Lett., 30, 2035, doi:10.1029/2003GL017861, 2003.

Edwards, D. P., Emmons, L. K., Gille, J. C., Chu, A., Attié, J. L., Giglio, L., Wood, S. W., Haywood, J., Deeter, M. N., Massie, S. T., Ziskin, D. C., and Drummond, J. R.: Satellite observed pollution from Southern Hemisphere biomass burning, J. Geophys. Res.-Atmos., 111, D14312, doi:10.1029/2005JD006655, 2006.

Feng, N. and Christopher, S. A.: Clear sky direct radiative effects of aerosols over Southeast Asia based on satellite observations and radiative transfer calculations, Remote Sens. Environ., 152, 333–344, 2014.

Freitas, S. R., Longo, K. M., Silva Dias, M. A. F., Silva Dias, P. L., Chatfield, R., Prins, E., Artaxo, P., and Recuero, F. S.: Monitoring the transport of biomass burning emissions in South America, Environ. Fluid Mech., 5, 135–167, doi:10.1007/s10652-005-0243-7, 2005.

Halthore, R., Eck, T., Holben, B., and Markham, B.: Sun photometric measurements of atmospheric water vapor column abundance in the 940-nm band, J. Geophys. Res., 102, 4343–4352, 1997.

Haywood, J. and Boucher, O.: Estimates of the direct and indirect radiative forcing due to tropospheric aerosols: a review, Rev. Geophys., 38, 513–543, doi:10.1029/1999RG000078, 2000.

Holben, B. N., Setzer, A., Eck, T. F., Pereira, A., and Slutsker, I.: Effect of dry-season biomass burning on Amazon basin aerosol concentrations and optical properties, 1992–1994, J. Geophys. Res.-Atmos., 101, 19465–19481, doi:10.1029/96jd01114, 1996.

Holben, B. N., Eck, T. F., Slutsker, I., Tanre, D., Buis, J. P., Setzer, A., Vermote, E., Reagan, J. A., Kaufman, Y. J., Nakajima, T., Lavenu, F., Jankowiak, I., and Smirnov, A.: AERONET – a federated instrument network and data archive for aerosol characterization, Remote Sens. Environ., 66, 1–16, doi:10.1016/S0034-4257(98)00031-5, 1998.

King, M. D., Kaufman, Y. J., Menzel, W., and Tanre, D.: Remote sensing of cloud, aerosol, and water vapor properties from the Moderate Resolution Imaging Spectrometer (MODIS), IEEE T. Geosci. Remote, 30, 2–27, 1992.

Koren, I., Martins, J. V., Remer, L. A., and Afargan, H.: Smoke invigoration versus inhibition of clouds over the Amazon, Science, 321, 946–949, 2008.

Liou, K. N.: An Introduction to Atmospheric Radiation, Vol. 84, Academic Press, San Diego, California, 2002.

Loeb, N. G. and Su, W.: Direct aerosol radiative forcing uncertainty based on a radiative perturbation analysis, J. Climate, 23, 5288–5293, 2010.

Loeb, N. G., Kato, S., Loukachine, K., and Manalo-Smith, N.: Angular distribution models for top-of-atmosphere radiative flux estimation from the Clouds and the Earth's Radiant Energy System instrument on the Terra satellite. Part I: Methodology, J. Atmos. Ocean. Tech., 22, 338–351, doi:10.1175/JTECH1712.1, 2005.

Loeb, N. G., Kato, S., Loukachine, K., Manalo-Smith, N., and Doelling, D. R.: Angular distribution models for top-of-atmosphere radiative flux estimation from the Clouds and the Earth's Radiant Energy System instrument on the Terra satellite. Part II: Validation, J. Atmos. Ocean. Tech., 24, 564–584, doi:10.1175/JTECH1983.1, 2007.

Longo, K., de Freitas, S. R., Andreae, M. O., Yokelson, R., and Artaxo, P.: Biomass burning in Amazonia: emissions, long-range transport of smoke and its regional and remote impacts, in: Amazonia and Global Change, edited by: Keller, M., Bustamante, M., Gash, J., and Dias, P. S., American Geophysical Union, Washington, D. C., Geophysical Monograph 186, 209–234, ISBN: 978-0-87590-449-8, doi:10.1029/2008GM000778, 2009.

Lucht, W., Schaaf, C. B., and Strahler, A. H.: An algorithm for the retrieval of albedo from space using semiempirical BRDF models, IEEE T. Geosci. Remote, 38, 977–998, doi:10.1109/36.841980, 2000.

Martin, S. T., Andreae, M. O., Artaxo, P., Baumgardner, D., Chen, Q., Goldstein, A. H., Guenther, A. B., Heald, C. L., Mayol-Bracero, O. L., McMurry, P. H., Pauliquevis, T., Pöschl, U., Prather K. A., Roberts G. C., Saleska S. R., Silva Dias M. A., Spracklen D. V., Swietlicki E., and Trebs I.: Sources and properties of amazonian aerosol particles, Rev. Geophys., 48, RG2002, doi:10.1029/2008RG000280, 2010.

Patadia, F. and Christopher, S. A.: Assessment of smoke shortwave radiative forcing using empirical angular distribution models, Remote Sens. Environ., 140, 233–240, 2014.

Patadia, F., Gupta, P., Christopher, S. A., and Reid, J. S.: A Multisensor satellite-based assessment of biomass burning aerosol radiative impact over Amazonia, J. Geophys. Res, 113, D12214, doi:10.1029/2007JD009486, 2008.

Patadia, F., Christopher, S. A., and Zhang, J.: Development of empirical angular distribution models for smoke aerosols: methods, J. Geophys. Res.-Atmos., 116, 1984–2012, 2011.

Prins, E. M., Feltz, J. M., Menzel, W. P., and Ward, D. E.: An overview of goes-8 diurnal fire and smoke results for scar-b and 1995 fire season in South America, J. Geophys. Res.-Atmos., 103, 31821–31835, 1998.

Procopio, A., Artaxo, P., Kaufman, Y., Remer, L., Schafer, J., and Holben, B.: Multiyear analysis of Amazonian biomass burning smoke radiative forcing of climate, Geophys. Res. Lett., 31, L03108–L03112, doi:10.1029/2003GL018646, 2004.

Remer, L. A., Kaufman, Y., Tanré, D., Mattoo, S., Chu, D. A., Martins, J. V., Li, R., Ichoku, C., Levy, R., Kleidman, R., Eck, T. F., Vermote, E., and Holben, B. N.: The MODIS aerosol algorithm, products and validation, J. Atmos. Sci., 62, 947–973, 2005.

Ricchiazzi, P., Yang, S., Gautier, C., and Sowle, D.: SBDART: a research and teaching software tool for plane-parallel radiative transfer in the Earth's atmosphere, B. Am. Meteorol. Soc., 79, 2101–2114, 1998.

Ross, J., Hobbs, P., and Holben, B.: Radiative characteristics of regional hazes dominated by smoke from biomass burning in Brazil: closure tests and direct radiative forcing, J. Geophys. Res., 103, 31,925–31, 1998.

Salomonson, V. V., Barnes, W., Maymon, P. W., Montgomery, H. E., and Ostrow, H.: MODIS: advanced facility instrument for studies of the Earth as a system, IEEE T. Geosci. Remote, 27, 145–153, 1989.

Schaaf, C. B., Gao, F., Strahler, A. H., Lucht, W., Li, X., Tsang, T., Strugnell, N. C., Zhang, X., Jin, Y., Muller, J.-P., Lewis, P., Barnsley, M., Hobson, P., Disney, M., Dunderdale, M., Doll, C., d'Entremont, R. P., Hu, B., Liang, S., Privette, J. L., and Roy, D.: First operational BRDF, albedo nadir reflectance products from MODIS, Remote Sens. Environ., 83, 135–148, doi:10.1016/S0034-4257(02)00091-3, 2002.

Schafer, J. S., Eck, T. F., Holben, B. N., Artaxo, P., and Duarte, A.: Characterization of the optical properties of atmospheric aerosols in Amazonia from long term AERONET monitoring (1993–1995; 1999–2006), J. Geophys. Res.-Atmos., 113, D04204, doi:10.1029/2007JD009319, 2008.

Sena, E. T., Artaxo, P., and Correia, A. L.: Spatial variability of the direct radiative forcing of biomass burning aerosols and the effects of land use change in Amazonia, Atmos. Chem. Phys., 13, 1261–1275, doi:10.5194/acp-13-1261-2013, 2013.

Smith, G. L.: Effects of time response on the point spread function of a scanning radiometer, Appl. Optics, 33, 7031–7037, 1994.

Stamnes, K., Tsay, S., Wiscombe, W., and Jayaweera, K.: Numerically stable algorithm for discrete–ordinate-method radiative transfer in multiple scattering and emitting layered media, Appl. Optics, 27, 2502–2509, 1988.

Sundström, A.-M., Arola, A., Kolmonen, P., Xue, Y., de Leeuw, G., and Kulmala, M.: On the use of satellite remote sensing based approach for determining aerosol direct radiative effect over land: a case study over China, Atmos. Chem. Phys. Discuss., 14, 15113–15147, doi:10.5194/acpd-14-15113-2014, 2014.

Twomey, S.: The influence of pollution on the shortwave albedo of clouds, J. Atmos. Sci., 34, 1149–1152, 1977.

Wielicki, B. A., Barkstrom, B. R., Harrison, E. F., Lee, R. B., Smith, G. L., and Cooper, J. E.: Clouds and the Earth's Radiant Energy System (CERES): an Earth observing system experiment, B. Am. Meteorol. Soc., 77, 853–868, 1996.

Yu, H., Kaufman, Y. J., Chin, M., Feingold, G., Remer, L. A., Anderson, T. L., Balkanski, Y., Bellouin, N., Boucher, O., Christopher, S., DeCola, P., Kahn, R., Koch, D., Loeb, N., Reddy, M. S., Schulz, M., Takemura, T., and Zhou, M.: A review of measurement-based assessments of the aerosol direct radiative effect and forcing, Atmos. Chem. Phys., 6, 613–666, doi:10.5194/acp-6-613-2006, 2006.

Zhang, J., Christopher, S. A., Remer, L., and Kaufman, Y. J.: Shortwave aerosol radiative forcing over cloud-free oceans from Terra: 2. Seasonal and global distributions, J. Geophys. Res., 110, D10S24, doi:10.1029/2004JD005009, 2005.
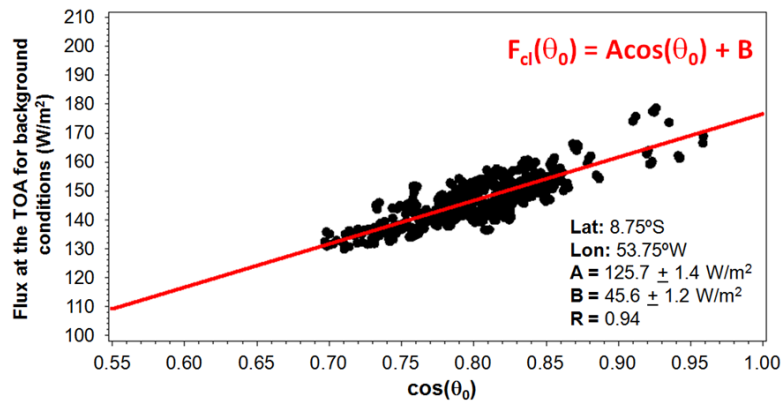
**Figure 1.** Example of the procedure used to obtain the flux at the top of the atmosphere (TOA) for background conditions ($F_{cl}$) as a function of the solar zenith angle ($\theta_0$) for a $0.5° \times 0.5°$ cell located in the Amazon Basin.
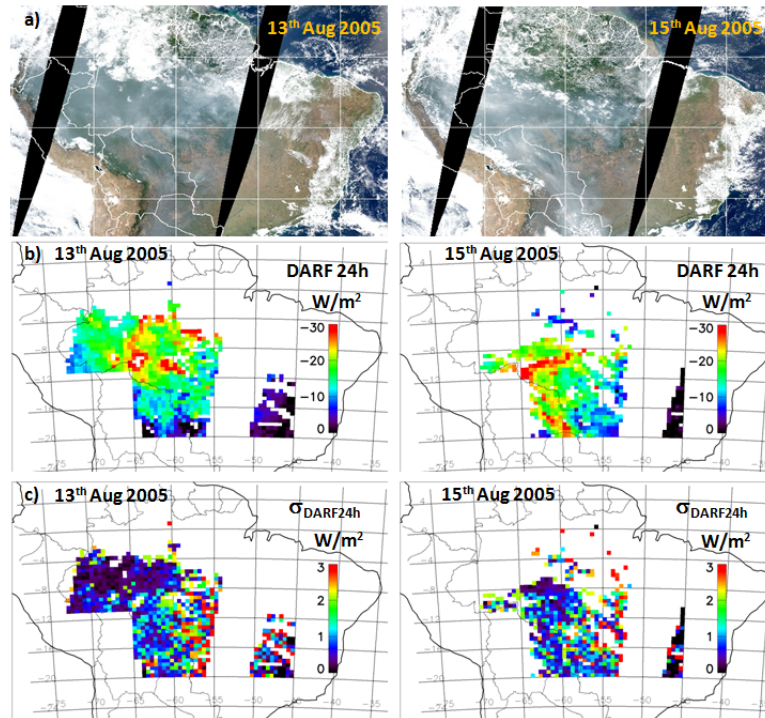
**Figure 2. (a)** Examples of composite MODIS RGB (red, green, blue) images over the Amazonia, **(b)** mean daily spatial distribuitions of the direct aerosol radiative forcing of aerosols (DARF24h), **(c)** and their uncertainties for 13 August 2005 (left) and 15 August 2005 (right).
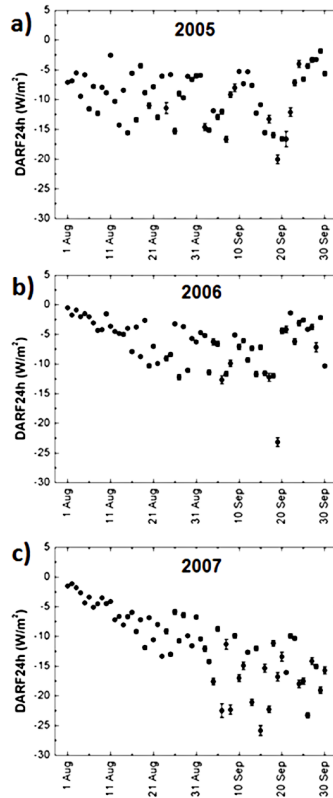
**Figure 3.** Temporal variability of the direct radiative forcing of aerosols (DARF24h) along the biomass burning season for: **(a)** 2005, **(b)** 2006 and **(c)** 2007.
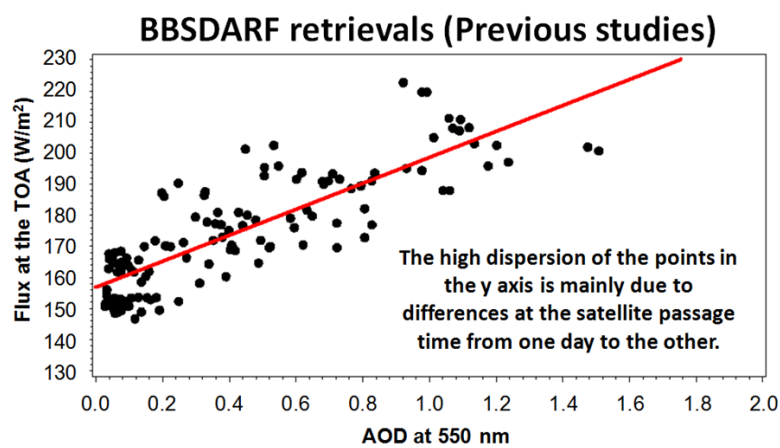
**Figure 4.** Example of the methodology previously used (eg., by Patadia et al., 2008 and Sena et al., 2013) to estimate the average of the DARF during the biomass burning season (BBS-DARF) using CERES and MODIS sensors.
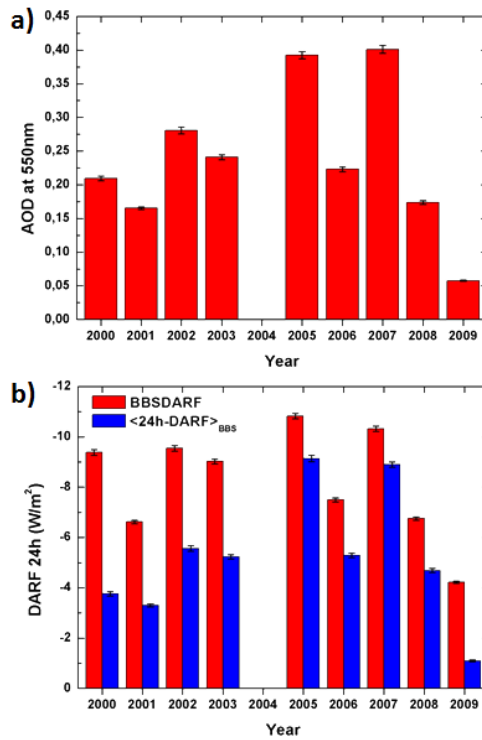
**Figure 5. (a)** MODIS mean aerosol optical depth at 550 nm over Amazonia during the dry season **(b)** and mean direct aerosol radiative forcing of aerosols (DARF24h) during the peak of the biomass burning season (August to September) from 2000 to 2009 obtained by the methodology applied by Sena et al., 2013 (BBSDARF) and by the methodology proposed in this work ($\langle$24hDARF$\rangle_{BBS}$).
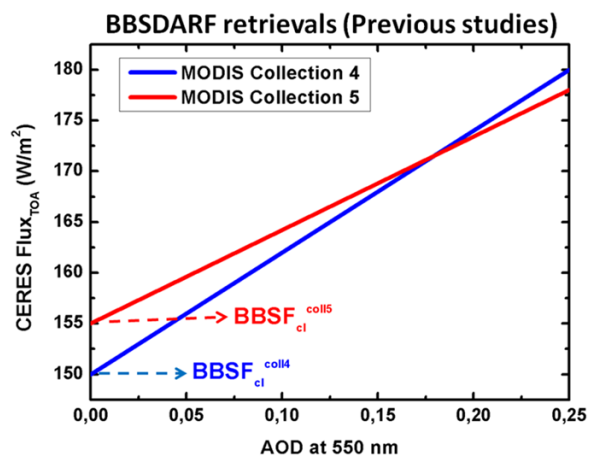
**Figure 6.** Schematic illustration of the differences in the linear fits of CERES flux at the top of the atmosphere (TOA) and MODIS collection 4 and collection 5 aerosol optical depth (AOD) at 550 nm.
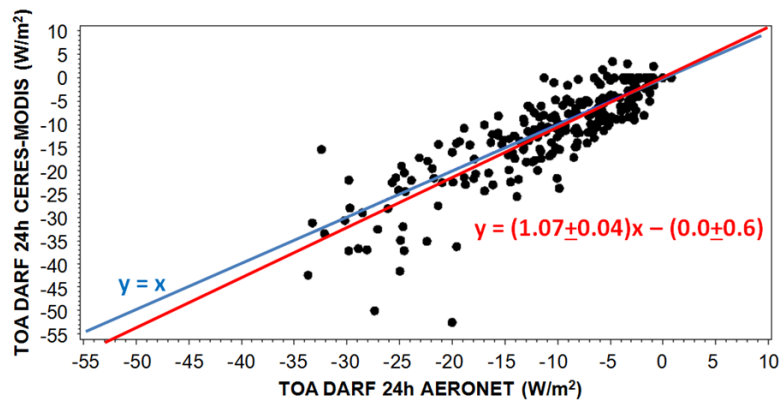
**Figure 7.** Intercomparison between the mean daily direct radiative forcing (DARF24h) at the top of the atmosphere (TOA) evaluated using CERES-MODIS and by AERONET inversion product.

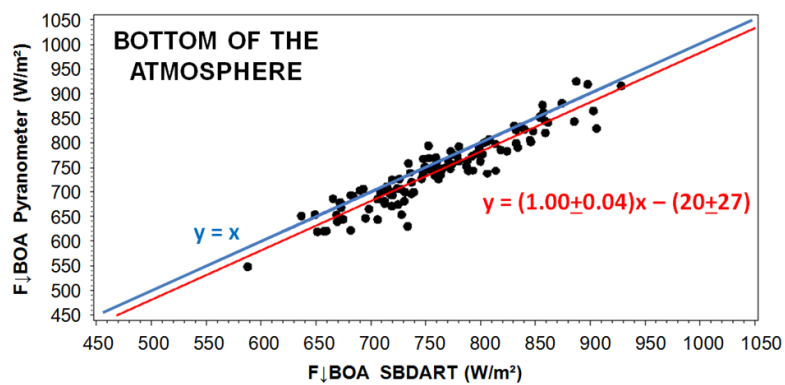**Figure 8.** Intercomparison between the incoming flux in $W\,m^{-2}$ at the bottom of the atmosphere (BOA) measured by SolRad-NET pyranometers and modelled using AERONET and MODIS BRDF retrieved optical properties as inputs in SBDART.
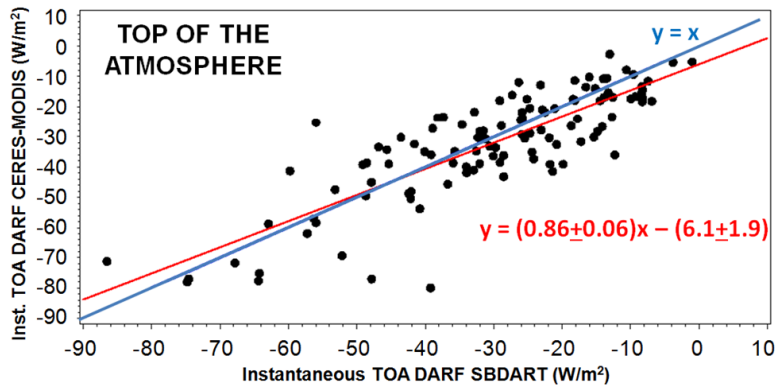
**Figure 9.** Intercomparison between the instantaneous direct aerosol radiative forcing (DARF) at the top of the atmosphere (TOA) evaluated using CERES-MODIS and modelled using AERONET and MODIS BRDF retrieved optical properties as inputs in SBDART.
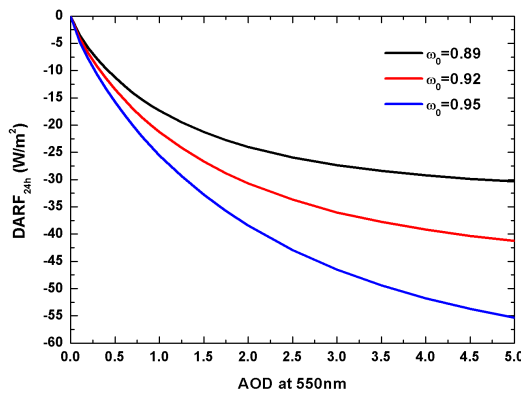
**Figure 10.** Direct radiative forcing of biomass burning aerosols (DARF24h) over the forest as a function of aerosol optical depth (AOD) at 550 nm and single scattering albedo ($\omega_0$) at 440 nm according to radiative transfer calculations.